Fusion Engineering and Design 83 (2008) 1082–1086

Contents lists available at ScienceDirect

Fusion Engineering and Design

journal homepage: www.elsevier.com/locate/fusengdes

Experimental study of MHD effects on turbulent flow of Flibe simulant fluid in circular pipe

Junichi Takeuchi[a,*], Shin-ichi Satake[b], Neil B. Morley[a], Tomoaki Kunugi[c], Takehiko Yokomine[d], Mohamed A. Abdou[a]

[a] Mechanical and Aerospace Engineering Department, Univeristy of California, Los Angeles, 420 Westwood Plaza, 44-114 Engineering IV, Los Angeles, CA 90095, USA
[b] Department of Applied Electronics, Tokyo University of Science, 2641 Yamazaki, Noda, Chiba 278-8510, Japan
[c] Department of Nuclear Engineering, Kyoto University, Yoshida, Sakyo, Kyoto 606-8501, Japan
[d] Interdisciplinary Graduate School of Engineering Science, Kyushu University, 6-1 Kasuga-koen, Kasuga, Fukuoka 816-8580, Japan

ARTICLE INFO

Article history:
Available online 5 November 2008

Keywords:
MHD
Flibe
Turbulent pipe flow
PIV

ABSTRACT

An investigation of MHD effects on a Flibe (Li_2BeF_4) simulant fluid has been conducted under the U.S.–Japan JUPITER-II collaboration program using the "FLIHY" pipe flow facility at UCLA. The present paper reports experimental results on turbulent pipe flow of an aqueous potassium hydroxide solution under magnetic field using particle image velocimetry (PIV) technique. The modification of turbulence was investigated by comparison of the experimental results with a direct numerical simulation (DNS) data base. The PIV measurements at Re = 11,300 were performed with variable Hartmann numbers, and the modification of the mean flow velocity as well as turbulence reduction was observed. A flat velocity profile in the pipe center and a steep velocity gradient in the near-wall region exhibit typical characteristics of wall-bounded MHD flows. The DNS was performed approximately the same conditions and the comparison of turbulence statistics between PIV and DNS shows good agreement for up to Ha = 10.

1. Introduction

The design of tritium breeding blankets and plasma facing components is an important area of R&D activities toward a viable commercial nuclear fusion reactor. In recent research, a molten salt coolant, Flibe (Li_2BeF_4), has attracted attention. Moriyama et al. [1] surveyed various design concepts using Flibe and suggested its use in reactor designs where high temperature stability and low MHD pressure drop were special concerns. Among the design concepts utilizing Flibe are HYLIFE-II [2], the APEX thick/thin liquid walls [3], FFHR [4], and a solid first wall design based on advanced nanocomposite ferritic steel [5]. Although Flibe has attractive features as coolant and tritium breeding material, there are some issues making Flibe-based blanket design challenging [5]. The main issues include (1) thermal conductivity of Flibe (1 W/mK) is low compared to other lithium-containing metal alloys, Pb–17Li (15 W/mK) and Li (50 W/mK), (2) kinematic viscosity of Flibe is high, especially at temperatures close to the melting point (11.5×10^{-6} m^2/s at 500 °C), and (3) the high melting point of Flibe requires structural material with temperature range over 650 °C.

The limited operating temperature window of Flibe coolant requires good heat transfer from heated surface to the bulk flow. However, the high viscosity and low thermal conductivity put Flibe in the class of high Prandtl number fluids. In order to obtain sufficiently large heat transfer using high Prandtl number fluid coolant, strong turbulence is required. On the other hand, Wong et al. [5] suggested that the parameter Ha/Re would exceed the critical value of 0.008 given by Branover [6], especially in large channels, which indicated the suppression of turbulence might be significant.

In this paper, the Reynolds number is defined as $\mathrm{Re} = U_b D/\nu$, and the Hartmann number as $\mathrm{Ha} = BR\sqrt{\sigma/\rho\nu}$ where U_b, D, ν, B, R, σ and ρ are mean velocity, pipe diameter, kinematic viscosity, magnetic flux density, pipe radius, electrical conductivity and fluid density, respectively. Comparisons of typical non-dimensional parameters between the current experiments and the design proposed by Wong et al. [5] are shown in Table 1.

The MHD effects on turbulent flows have been investigated extensively; however, most of the experimental efforts were conducted using liquid metals as working fluids [7,8]. Liquid metals are generally classified as low Prandtl number fluids, and the heat transfer characteristics of low Prandtl number fluids are conduction dominant. However, the MHD effects on high Prandtl number, low conductivity fluids are yet to be understood. Thus it is important to investigate the effect of magnetic fields on the turbulent

* Corresponding author. Tel.: +1 310 794 4452; fax: +1 310 825 2599.
E-mail address: takeuchi@fusion.ucla.edu (J. Takeuchi).

0920-3796/$ – see front matter © 2008 Elsevier B.V. All rights reserved.
doi:10.1016/j.fusengdes.2008.08.050

Table 1
Comparison of typical dimensionless parameters for the present experiment with molten salt blanket [5].

	Ha	Re	Ha/Re	$N(=Ha^2/Re)$
Experiment	20	11,300	1.8×10^{-3}	3.5×10^{-2}
Self-cooled fusion blanket	20	12,000	1.7×10^{-3}	3.3×10^{-2}

flow and heat transfer characteristics of the high Prandtl number fluids.

To understand the underlying phenomena controlling the fluid mechanics and heat transfer of Flibe, a series of experiments as a part of the U.S.–Japan JUPITER-II collaboration has been conducted. The approach includes flow and heat transfer measurements using a Flibe simulant fluid along with numerical simulation and modeling. In the preceding research, free surface flows were investigated through experiments and modeling [9,10]. In the present phase, a flow facility utilizing water and aqueous electrolytes as Flibe simulants has been constructed, and flows in a close channel are being investigated. Turbulent flow field measurements using PIV [11] and heat transfer measurements [12] have been carried out without magnetic field to establish the experimental techniques and verify the performance of the facility by comparing an existing experimental result [13] and DNS data [14]. The development of the experimental techniques under magnetic fields was described in a previous report [15]. A modeling effort has also been performed by Smolentsev et al. [16].

The objective of the present study is to investigate the modification of the turbulence structures of the MHD turbulent pipe flow by comparing the experimental results obtained by PIV with DNS under the same flow conditions [17,18]. The PIV measurements yield velocity data in the plane parallel to the bulk flow and the field direction, and the turbulence statistics are calculated from 5000 image pairs. The spacial structures are also observed. Since most of the existing experimental data of MHD turbulent flows were obtained with liquid metals, flow visualization was impossible. The present work provides unique 2-dimensional 2-velocity-component information of the flow field to improve understandings of the MHD turbulent flows.

2. Experiments

An experimental MHD flow facility called "FLIHY" (Flibe Hydrodynamics) has been constructed at UCLA. The experimental facility consists of a closed channel flow loop with a circular pipe test section and integrated transparent visualization section, a magnet system, and a PIV measurement system. A 30% aqueous solution of potassium hydroxide (KOH hereafter) is used as the electrically conducting working fluid.

2.1. Experimental apparatus

A schematic drawing of the pipe flow apparatus is shown in Fig. 1. The fluid flow is circulated by a pump and introduced into the horizontal circular pipe test section. Flow passes through a heat exchanger, a flow meter, and a honeycomb flow straightener before entering the test section. The temperature of the fluid is monitored by thermocouples and kept constant using the heat exchanger. The test section is a circular pipe made of acrylic with 89 mm inner diameter and 7.0 m in length, which is 79 times the pipe diameter. This length is considered to be sufficient to obtain a fully developed turbulent flow. This relatively large diameter was chosen to allow access to information in near-wall region by making viscous length scale large. The flow rate is controlled by changing the pump output with a variable frequency power controller. A throttle valve in the

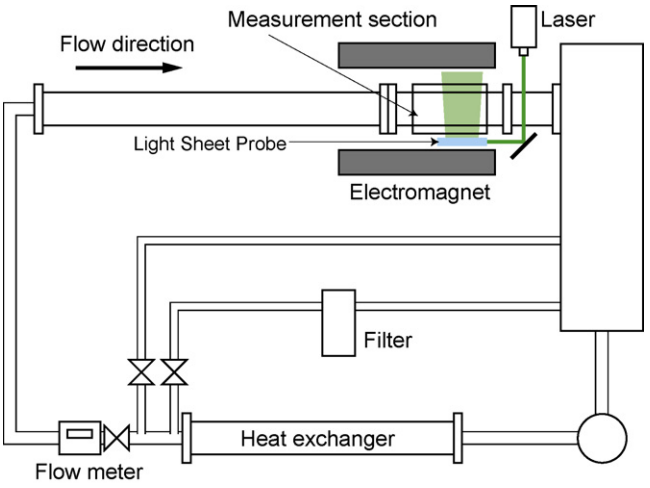

Fig. 1. Experimental apparatus.

main loop and a bypass line are also equipped to help flow rate control. The flow rate is measured and monitored by vortex-shedding flow meter [19]. The visualization section for the PIV measurement was built 6.8 m downstream from the inlet. The pipe wall thickness in the visualization section is 1 mm to allow velocity measurement down to very close to the pipe wall. A "water jacket" tank with square cross-section was installed surrounding the pipe. The cross-section view of the water jacket is shown in Fig. 2. The water jacket is 11 cm × 11 cm in the cross-section and 23 cm long and is filled with the same fluid as the main flow in order to compensate for the image distortion due to the difference in index of refraction between inside and outside of the circular pipe. This eliminates the optical distortion to a negligible level.

2.2. Magnet

The magnet used for the current experiments produces maximum 2.0 T magnetic fields in a narrow gap of the iron core at 3000 A

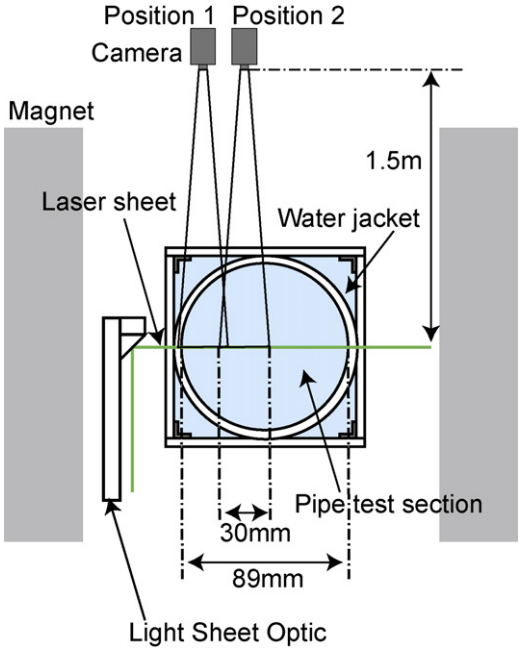

Fig. 2. Cross-section view of measurement section.

of applied electric current. The pipe flow test section was placed in the gap which is 1.4 m in the streamwise direction, 25 cm in height, and 15 cm in width. The B field has uniform distribution within 5% variation for 1.0 m in the streamwise direction. There was no direct proof showing the flow development length under the magnetic field was sufficient to fully establish the MHD effects; however, the 11 diameter development length was estimated based on the DNS [17]. The time required to obtain fully developed MHD flow multiplied by the mean velocity gave approximately 10 diameters. The fact that the time scale of Joule damping [20] $\tau_j = \rho/\sigma B^2 \sim 3.8$ [s] was small compared to the time required for the fluid to travel from the inlet to the measurement point ~7.0 [s] also supported this consideration. However, this flow development length is smaller than that of Reed and Lykoudis [8] in which the length was 20 times hydraulic diameter.

2.3. PIV system

The PIV technique has been developed in last two decades and has become a well established technique for flow field measurements [21]. Seeding particles were selected so that they are compatible with KOH and their density was comparable to that of KOH (1300 kg/m^3). Methyl methacrylate–ethylene glycol dimethacylate copolymer (Sekisui Plastic Co., Ltd.) turned out to be compatible as well as to have the density close to the solution (about 1200 kg/m^3). Although it was not specifically tailored for PIV use, its relatively uniform particle diameter (5 μm) was suitable for PIV measurements.

A laser beam supplied by New Wave Solo-III Nd:YAG Laser is introduced into the magnet gap using a dielectric coated mirror. Light sheet optic placed in the magnet gap converts the laser beam into a thin sheet less than 1 mm in thickness with a cylindrical lens and introduces it horizontally to the measurement plane with two dielectric mirrors. The particle images illuminated by the laser sheet are captured by Phantom v.5.0 high speed camera (Vision Research Inc.). The camera has 1024 × 1024 pixels monochrome CMOS array. A Tamron SP 35–210 mm lens is used along with extension tubes to achieve 90 mm × 90 mm and 30 mm × 30 mm field of view on the measurement plane 1.0 m from the lens.

Dantec FlowManager 3.70 software is used for PIV analysis. It provides analysis method called “adaptive correlation”, which is based on commonly used cross-correlation technique [22]. The important feature of the adaptive correlation is a multiple step analysis method [23]. Large interrogation windows are used in the first step and the interrogation windows are successively reduced in the following steps. For this experiment, the reduction of the window size is repeated 4 times. Thus 256 × 128 pixels interrogation windows in the first step are reduced to 32 × 16 pixels in the final step. In each step, a cross-correlation analysis is performed twice. The first analysis gives a rough estimate of the particle displacement by analyzing exactly the same area in the first and second images. This information is used then to determine the location of the interrogation windows for the second analysis in order to minimize loss of particle pairs in the windows [24]. To reduce the possibility of yielding spurious vectors due to mismatch of the particle pairs, local median validation is applied between the steps, and the invalidated vectors are replaced by using information from the vectors in vicinity [25]. The particle displacement was determined down to sub-pixel order. A Dantec 80S33 high accuracy software module is used for this experiment. This module has an advantage over the conventional three-point Gaussian curve fitting method; however, access to the detail of the algorithm is prevented by proprietary information issue.

Table 2
Thermophysical properties of aqueous KOH solution and Flibe.

		KOH solution (33.8 °C)	Flibe (600 °C)
ρ	Density (kg/m^3)	1.28×10^3	2.12×10^3
μ	Viscosity (Pa s)	1.431×10^{-3}	11.6×10^{-3}
ν	Kinematic viscosity (m^2/s)	1.118×10^{-6}	5.48×10^{-6}
σ	Electrical conductivity (S/m)	73.67	155
λ	Heat conductivity (W/(m K))	0.727	1.00
C_p	Heat capacity (J/(kg K))	3.00×10^3	2.34×10^3
Pr	Prandtl number	5.90	28

2.4. Thermophysical properties of KOH solution

In order to determine the thermo-physical properties of 30% KOH aqueous solution, measurements were carried out for some of the most critical of them. The kinematic viscosity was measured by U-tube capillary viscometer. The electrical conductivity was measured by conductivity meter. Other properties were quoted from a reference book [26]. Table 2 shows the thermo-physical properties of KOH solution at 33.8 °C experimental temperature and that of Flibe at 600 °C.

3. Results and discussion

PIV measurements are performed for Re = 11,300 with variable Hartmann numbers. The measurements are performed in the plane parallel to the magnetic field. The turbulence statistics for the experimental data are calculated from 5000 image pairs, and the results are compared with the available direct numerical simulation data [17,18].

3.1. Mean velocity

Fig. 3 shows the comparison of the mean velocity profiles normalized by centerline velocity. In the plane parallel to the magnetic field, the pipe wall is perpendicular to the field. Therefore, the wall is considered to be a Hartmann wall. The velocity gradient gets steeper along the wall perpendicular to the magnetic field and flatter in core region. This is a typical characteristics of the wall-bounded MHD flows. The figure shows good agreement in mean velocity profiles between experimental data and numerical simulations and the discrepancy is within the measurement uncertainty of 2%.

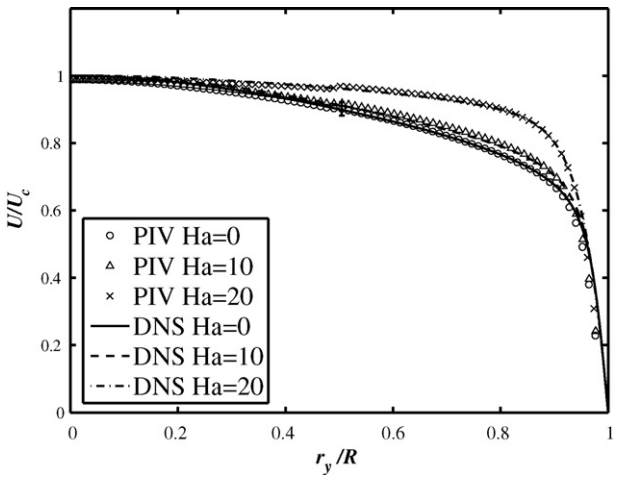

Fig. 3. Mean velocity distributions at Re = 11,300 normalized by center line velocity.

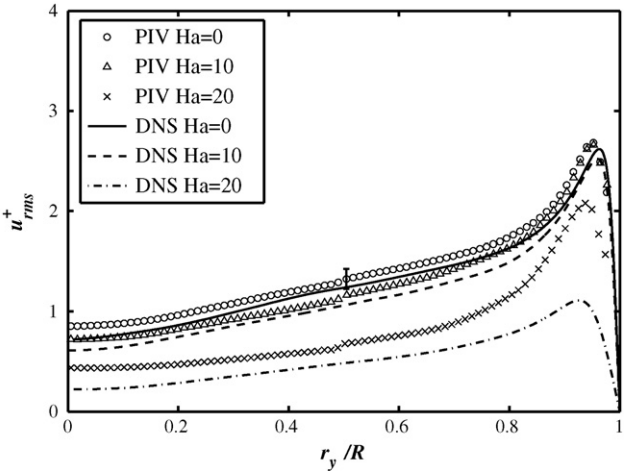

Fig. 4. Streamwise turbulence intensities distributions at Re = 11,300 normalized by friction velocity for hydrodynamical case.

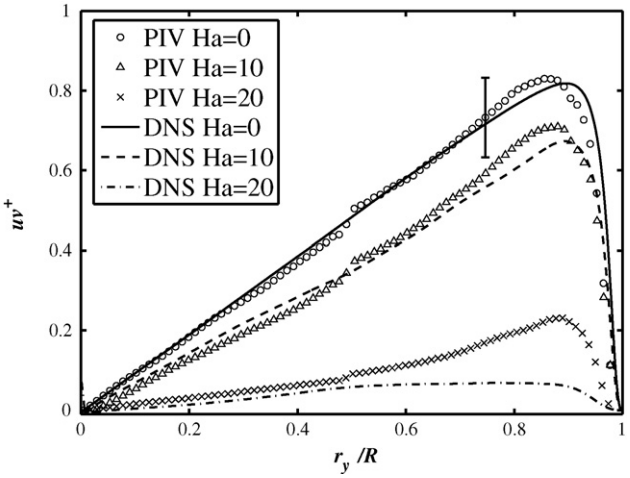

Fig. 6. Reynolds shear stress distributions at Re = 11,300 normalized by square of friction velocity for hydrodynamical case.

3.2. Turbulence intensities

Figs. 4 and 5 show root-mean-square velocity (turbulence intensity) profile normalized by friction velocity at Ha = 0 (hydrodynamical case) in the streamwise direction and in the radial direction parallel to the B field, respectively. For Ha = 5, no significant change compared to the hydrodynamical case was observed in both components (not shown). For Ha = 10, the streamwise turbulence intensity in the core region decreases by 19% compared to hydrodynamical case; however, near-wall peak remains the same level. The radial turbulence intensity also decreases by 19% in the core region, and on the contrary to the streamwise direction, the near-wall peak decreases in this direction. The experimental data show slightly higher value compared to DNS; however, the discrepancy is considered to be within the measurement uncertainty of 10% of the friction velocity. Although the mean velocity profiles at Ha = 20 agree between the experiment and simulation, significant discrepancy in the turbulence intensities is found for Ha = 20. In the near-wall peak of the streamwise turbulence intensity, the experimental data show almost twice as large as the DNS data.

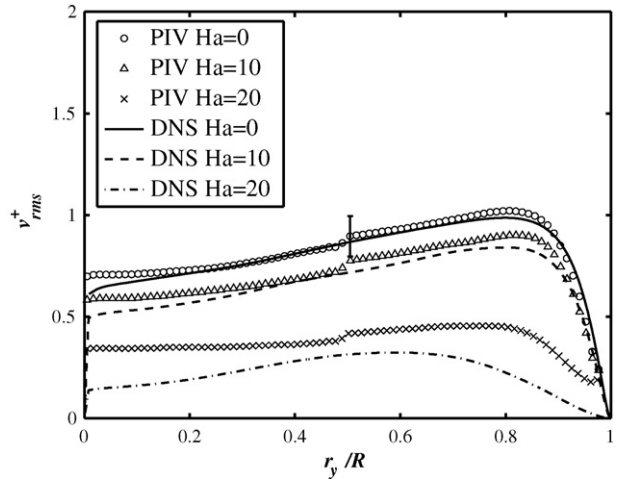

Fig. 5. Radial turbulence intensities distributions parallel to the B field at Re = 11,300 normalized by friction velocity for hydrodynamical case.

3.3. Reynolds shear stress

Fig. 6 shows the Reynolds shear stress distributions normalize by square of the friction velocity. For Ha = 10, the Reynolds stress at the peak decreases by 16% for both PIV and DNS compared to the one for Ha = 0. Good agreement between the experiment and DNS is obtained for this case. For Ha = 20, the experimental data coincide with DNS in the core region whereas a significant discrepancy is seen in near-wall region. The discrepancy between the experimental results and DNS may be due to insufficient flow development length. It is also conjectured that differences in the inlet condition of the magnetic region may have some effect for these cases. In the experiment, the magnetic field was suddenly applied when the fluid enters the magnetic region; however, in the DNS, the field strength was gradually increased with the time advancement. Finally, it may be that we are near a cliff for sharp decrease in turbulence, as shown by Gardner and Lykoudis [7] around Ha = 20–25. Therefore, small errors in Hartmann number and Reynolds number could shift us beyond this cutoff.

4. Conclusions

The PIV measurements on turbulent pipe flow of aqueous KOH solution under magnetic field have been performed and MHD effects are investigated by comparing the turbulece statistics for the experimental results against DNS database. The mean velocity profiles between the experimental data and the DNS agree well within the measurement uncertainty up to Ha = 20. The turbulence intensities and Reynolds shear stress profiles for the experiment and DNS agree up to Ha = 10. The agreement between the experimental data and DNS data provides basis for evaluating the turbulence suppression in the fusion reactor design. As for the turbulence intensities and Reynolds shear stress for Ha = 20, the discrepancies between the experimental data and DNS are significantly large. In this Ha/Re range, sharp decrease in the turbulence quantities is expected based on the observation by Gardner and Lykoudis [7]. Therefore, it is expected that the small errors in the experimental parameters cause relatively large difference. The issue remains open for discussions.

Acknowledgements

Authors are grateful for the financial support from the U.S. D.O.E., Grant No. DE-FG03-86ER52123, and the Japanese Ministry

of Education, Culture, Sports, Science and Technology via JUPITER-II collaboration.

References

[1] H. Moriyama, A. Sagara, S. Tanaka, R.W. Moir, D.K. Sze, Molten salts in fusion nuclear technology, Fusion Engineering and Design 39–40 (1998) 627–637.
[2] R.W. Moir, R.L. Bieri, X.M. Chen, T.J. Dolan, M.A. Hoffman, P.A. House, R.L. Leber, J.D. Lee, Y.T. Lee, J.C. Liu, G.R. Longhurst, W.R. Meier, P.F. Peterson, R.W. Petzoldt, V.E. Schrock, M.T. Tobin, W.H. Williams, HYLIFE-II a molten salt inertial fusion energy power plant design—final report, Fusion Technology 25 (1) (1994) 5–25.
[3] M.A. Abdou, The APEX team, A. Ying, N. Morley, K. Gulec, S. Smolentsev, M. Kotschenreuther, S. Malang, S. Zinkle, T. Rognlien, P. Fogarty, B. Nelson, R. Nygren, K. McCarthy, M.Z. Youssef, N. Ghoniem, D. Sze, C. Wong, M. Sawan, H. Khater, R. Woolley, R. Mattas, R. Moir, S. Sharafat, J. Brooks, A. Hassanein, D. Petti, M. Tillack, M. Ulrickson, T. Uchimoto, On the exploration of innovative concepts for fusion chamber technology, Fusion Engineering and Design 54 (2001) 181–247.
[4] A. Sagara, O. Motojima, S. Imagawa, O. Mitarai, T. Noda, T. Uda, K. Watanabe, H. Yamanishi, H. Chikaraishi, A. Kohyama, H. Matsui, T. Muroga, N. Noda, N. Ohyabu, T. Satow, A.A. Shishkin, D.K. Sze, A. Suzuki, S. Tanaka, T. Terai, K. Yamazaki, J. Yamamoto, Design studies of helical-type fusion reactor FFHR, Fusion Engineering and Design 41 (1998) 349–355.
[5] C.P.C. Wong, S. Malang, M. Sawan, I. Sviatoslavsky, E. Mogahed, S. Smolentsev, S. Majumdar, B. Merrill, R. Mattas, M. Friend, J. Bolin, S. Sharafat, Molten salt self-cooled solid first wall and blanket design based on advanced ferritic steel, Fusion Engineering and Design 72 (2004) 245–275.
[6] H. Branover, Magnetohydrodynamic Flow in Ducts, Halsted Press, 1978, p. 156.
[7] R.A. Gardner, P.S. Lykoudis, Magneto-fluid mechanic pipe flow in a transverse magnetic field. Part 1. Isothermal flow, Journal of Fluid Mechanics 47 (1971) 737–764.
[8] C.B. Reed, P.S. Lykoudis, The effect of a transverse magnetic field on shear turbulence, Journal of Fluid Mechanics 89 (1) (1978) 147–171.
[9] S. Smolentsev, M.A. Abdou, N.B. Morley, A. Ying, T. Kunugi, Application of the "k-ϵ" model to open channel flows in a magnetic field, International Journal of Engineering Science 40 (2002) 693–711.
[10] S. Smolentsev, N.B. Morley, B. Freeze, R. Miraghaie, J.C. Nave, S. Banerjee, A. Ying, M.A. Abdou, Thermofluid modeling and experiments for free surface flows of low-conductivity fluid in fusion systems, Fusion Engineering and Design 72 (2004) 63–81.
[11] J. Takeuchi, S. Satake, N.B. Morley, T. Yokomine, T. Kunugi, M.A. Abdou, PIV measurements of turbulence statistics and near-wall structure of fully developed pipe flow at high reynolds number, in: Proceedings of 6th International Symposium on Particle Image Velocimetry, Pasadena, California, September 21–23, 2005, 2005.
[12] J. Takeuchi, S. Satake, R. Miraghaie, K. Yuki, T. Yokomine, T. Kunugi, N.B. Morley, M.A. Abdou, Study of heat transfer enhancement/suppression for molten salt flows in a large diameter circular pipe: Part one—Benchmarking, Fusion Engineering and Design 81 (2006) 601–606.
[13] J.G.M. Eggels, F. Unger, M.H.W.J. Weiss, R.J. Adrian, R. Friedrich, F.T.M. Nieuwstadt, Fully developed turbulent pipe flow: a comparison between direct numerical simulation and experiment, Journal of Fluid Mechanics 268 (1994) 175–209.
[14] S. Satake, T. Kunugi, R. Himeno, High Reynolds number computation for turbulent heat transfer in a pipe flow, in: M. Valero, K. Joe, M. Kitsuregawa, H. Tanaka (Eds.), Lecture Notes in Computer Science 1940, Springer-Verlag, Berlin-Heidelberg, 2000, pp. 514–523.
[15] J. Takeuchi, S. Satake, T. Kunugi, T. Yokomine, N.B. Morley, M.A. Abdou, Development of PIV technique under magnetic fields and measurement of turbulent pipe flow of flibe simulant fluid, Fusion Science and Technology 52 (4) (2007) 860–864.
[16] S. Smolentsev, R. Miraghaie, M.A. Abdou, MHD effects on heat transfer in a molten salt blanket, Fusion Science and Technology 47 (2005) 559–563.
[17] S. Satake, T. Kunugi, S. Smolentsev, Direct numerical simulations of turbulent pipe flow in a transverse magnetic field, Journal of Turbulence 3 (2002) 20.
[18] S. Satake, T. Kunugi, K. Takase, Y. Ose, Direct numerical simulation of turbulent channel flow under a uniform magnetic field for large-scale structures at high reynolds number, Physics of Fluids 18 (2006) 125106.
[19] R.J. Goldstein, Fluid Mechanics Measurements, Hemisphere Publishing, 1983.
[20] R. Moreau, Magnetohydrodynamics, Kluwer Academic Press, 1990.
[21] M. Raffel, C.E. Willert, J. Kompenhans, Particle Image Velocimetry, Springer-Verlag, Berlin-Heidelberg, 1998.
[22] R.D. Keane, R.J. Adrian, Theory of cross-correlation analysis of PIV image, in: F. Nieuwstadt (Ed.), Flow Visualization and Image Analysis, Kluwer Academic Publishers, Netherlands, 1993, pp. 1–25.
[23] F. Scarano, M.L. Riethmuller, Iterative multigrid approach in piv image processing with discrete window offset, Experiments in Fluids 26 (1999) 513–523.
[24] J. Westerweel, D. Dabiri, M. Gharib, The effect of a discrete window offset on the accuracy of cross-correlation analysis of digital PIV recordings, Experiments in Fluids 23 (1997) 20–28.
[25] J. Westerweel, Efficient detection of spurious vectors in particle image velocimetry data, Experiments in Fluids 16 (1994) 236–247.
[26] A.L. Horvath, Handbook of Aqueous Electrolyte Solutions, Ellis Horwood, Chichester, 1985.